The American Journal of Pathology, Vol. 193, No. 7, July 2023

ELSEVIER

The American Journal of PATHOLOGY

ajp.amjpathol.org

METABOLIC, ENDOCRINE, AND GENITOURINARY PATHOBIOLOGY

Hyperglycemia Induces Tear Reduction and Dry Eye in Diabetic Mice through the Norepinephrine—α_1 Adrenergic Receptor—Mitochondrial Impairment Axis of Lacrimal Gland

Sai Zhang,* Qun Wang,*† Mingli Qu,* Qing Chen,‡ Xiaofei Bai,*† Zhenzhen Zhang,§ Qingjun Zhou,*† and Lixin Xie*†

From the State Key Laboratory Cultivation Base, Shandong Provincial Key Laboratory of Ophthalmology, Shandong Eye Institute of Shandong First Medical University, Qingdao; the Qingdao Eye Hospital of Shandong First Medical University,† Qingdao; the School of Clinical Medicine,‡ Weifang Medical University, Weifang; and the Medical College of Qingdao University,§ Qingdao, China*

Accepted for publication March 28, 2023.

Address correspondence to Qingjun Zhou, Ph.D. or Lixin Xie, M.D., Ph.D., State Key Laboratory Cultivation Base, Shandong Provincial Key Laboratory of Ophthalmology, Shandong Eye Institute of Shandong First Medical University, 5 Yan'erdao Rd., Qingdao 266071, China. E-mail: zhouqingjun@sdfmu.edu.cn or lxxie@sdfmu.edu.cn.

Dry eye syndrome is a common complication in diabetic patients with a prevalence of up to 54.3%. However, the pathogenic mechanisms underlying hyperglycemia-induced tear reduction and dry eye remain less understood. The present study indicated that both norepinephrine (NE) and tyrosine hydroxylase levels were elevated in the lacrimal gland of diabetic mice, accompanied by increased Fos proto-oncogene (c-FOS)$^+$ cells in the superior cervical ganglion. However, the elimination of NE accumulation by surgical and chemical sympathectomy significantly ameliorated the reduction in tear production, suppressed abnormal inflammation of the lacrimal gland, and improved the severity of dry eye symptoms in diabetic mice. Among various adrenergic receptors (ARs), the α_1 subtype played a predominant role in the regulation of tear production, as treatments of α_1AR antagonists improved tear secretion in diabetic mice compared with βAR antagonist propranolol. Moreover, the α_1AR antagonist alfuzosin treatment also alleviated functional impairments of the meibomian gland and goblet cells in diabetic mice. Mechanically, the α_1AR antagonist rescued the mitochondrial bioenergetic deficit, increased the mitochondrial DNA copy numbers, and elevated the glutathione levels of the diabetic lacrimal gland. Overall, these results deciphered a previously unrecognized involvement of the NE-α_1AR-mitochondrial bioenergetics axis in the regulation of tear production in the lacrimal gland, which may provide a potential strategy to counteract diabetic dry eye by interfering with the α_1AR activity. *(Am J Pathol 2023, 193: 913—926; https://doi.org/10.1016/j.ajpath.2023.03.015)*

Diabetes mellitus (DM) is a chronic multisystem disease, which involves major complications largely influenced by hyperglycemia.[1] According to the International Diabetes Federation, 537 million people experienced diabetes worldwide in 2021.[2] DM is mostly associated with specific pathology of the retina, renal glomerulus, and peripheral nerves.[3–5] Dry eye is a significant complication of diabetes, with a reported prevalence of up to 54.3%.[6,7] In the clinic, dry eye has been a more common complaint than corneal symptoms in diabetes.[8] Lacrimal glands (LGs) are exocrine organs that secrete the aqueous layer of the tear film, which is essential for lubrication and protection of the eye.[9,10] However, to date, the pathologic changes of LGs in diabetic dry eye remain to be fully understood.

The LG is distributed mainly by autonomic nerves (including sympathetic and parasympathetic branches) and sensory nerves.[11] Overwhelming evidence indicates that LG

Supported by the Shandong Provincial Key Research and Development Program 2021ZDSYS14 (L.X.); the National Natural Science Foundation of China 82070927 (Q.Z.); the Taishan Scholar Program tstp20221163 (Q.Z.); and the Academic Promotion Program and Innovation Project of Shandong First Medical University 2019ZL001 (L.X.) and 2019RC008 (Q.Z.).

Disclosures: None declared.

https://doi.org/10.1016/j.ajpath.2023.03.015

secretion is primarily controlled by the parasympathetic branch of the autonomic nervous system.[12–14] Electrical stimulation of the superior cervical sympathetic ganglion and exogenous delivery of sympathomimetics stimulate protein secretion.[15,16] However, the physiological role of the sympathetic innervation of the lacrimal gland has been questioned because its function is not altered in rabbits when innervation from the superior cervical ganglion is interrupted.[17] Recently, a study by Jin et al[18] using an elegant experimental murine model has confirmed that the sympathetic system is not involved in tear secretion. Furthermore, sympathetic neuronal activation is well known in diabetes, including its role in triggering myeloid progenitor proliferation and differentiation, and antagonizing insulin-stimulated muscle glucose disposal, resulting in increased cardiovascular complications.[19–22] However, the involvement of sympathetic stimulation in LGs and the interactions between LGs and sympathetic neurotransmitter norepinephrine (NE) in diabetes mellitus remain poorly understood.

The current study indicated a previously unreported regulation of diabetic dry eye by the NE–α_1 adrenergic receptor (AR) axis. Hyperglycemia induced NE release, suggesting the involvement of NE in diabetic dry eye. Sympathetic nerves pass through the superior cervical ganglion and are distributed around the face where the LG is located.[18,23] NE accumulation in LGs can be surgically and chemically eliminated by superior cervical sympathectomy and administration of 6-hydroxydopamine (6-OHDA), which is a neurotoxin that depletes peripheral sympathetic neurons.[18,22] Herein, the intervention with NE generation improved hyperglycemia-induced tear reduction and dry eye severity, including LG inflammation and corneal condition. Furthermore, LG expressed high amounts of α_1 and β ARs. By using several clinically available α_1AR blocker drugs, including prazosin, alfuzosin, terazosin, and doxazosin, and βAR blocker drug propranolol,[24,25] the adaptor α_1AR was found to protect LG and ocular surface homeostasis from hyperglycemia. Mechanistically, α_1AR antagonist alfuzosin rescued the mitochondrial bioenergetic deficit in diabetic LGs, accompanied by revertible mitochondrial DNA (mtDNA) copies, glutathione (GSH) levels, and mitochondrial morphologic changes. These important findings may help establish potential strategies to counteract tear reduction and diabetic dry eye by manipulating sympathetic activity.

Materials and Methods

Animals

Adult male C57BL/6 mice (aged 6 to 8 weeks) were purchased from SPF Biotechnology Co, Ltd (Beijing, China). After a week of domestication, all mice were designated into two groups [namely, the control group (n = 10) and the DM group (n = 100)]. Type 1 DM was generated by i.p. injection of 50 mg/kg streptozotocin (STZ; Sigma-Aldrich, St. Louis, MO) for 5 days. Mice with a blood glucose level of >16.7 mmol/L 1 week after the last injection were considered eligible diabetic mice. After 16 weeks of the final injection of STZ, diabetic mice were sacrificed and collected for this study. Animal experiments followed the Association for Research in Vision and Ophthalmology's Statement for Use of Animals in Ophthalmic and Vision Research and were approved by the Ethics Committee of Shandong Eye Institute (Qingdao, China).

Drug Treatments

After 16 weeks of STZ-induced diabetic treatment, mice were divided into diabetic vehicle control group (n = 20), DM + 6-OHDA group (n = 10), DM + prazosin group (n = 10), DM + propranolol group (n = 10), DM + alfuzosin group (n = 10), DM + terazosin group (n = 10), and DM + doxazosin group (n = 10), and treated with the following drugs. The 6-OHDA hydrobromide [75 mg/kg body weight (BW), dissolved in 0.1% ascorbic acid solution; Sigma] was administered intraperitoneally every day for 4 days. Mice received 0.1% ascorbic acid solution as vehicle control. Prazosin (1 mg/kg BW; HY-B0193; MCE, Shanghai, China) and propranolol (10 mg/kg BW; HY-B0573B; MCE) dissolved in double-distilled water were administered intraperitoneally every day for 7 days. Alfuzosin hydrochloride tablets (5 mg/kg BW; Lunan BETTER Pharmaceutical Co, Ltd, Shandong, China), prazosin hydrochloride tablets (5 mg/kg BW; Shanghai Xinyi Medicine Co, Ltd, Shanghai, China), terazosin hydrochloride tablets (5 mg/kg BW; Shanghai Abbott Pharmaceutical Co, Ltd, Shanghai, China), and doxazosin mesylate tablets (5 mg/kg BW; Pfizer Pharmaceuticals LLC, New York, NY) dissolved in double-distilled water were administered orally for 7 days. Mice received double-distilled water as vehicle control.

Superior Cervical Ganglionectomy

Diabetic mice were randomly divided into the superior cervical ganglionectomy (SCGx) group (n = 10) and the sham surgery group (n = 10). Mice were anesthetized with sodium pentobarbital (50 mg/kg) and placed in the supine position. Small straight scissors were used to carefully incise 2 cm of the cervical skin of the mice above the submandibular gland. The superior cervical ganglion adjacent to the carotid artery located at the medial side of the submandibular gland was excised, and the incised site was sutured. The sham group was obtained by exposing but not removing the superior cervical ganglion (SCG).

Tear Production Measurement

Tear secretion was determined by using the cotton thread test with standardized phenol red–impregnated cotton threads (30059010; Jingming, Tianjin, China). The evaluation of tear secretion was conducted by inserting a thread

under the lower eyelid for 20 seconds. The length of the wet portion was measured in millimeters.

Corneal RB Staining and Scores

Corneal Rose Bengal (RB) staining was used to visualize and quantify dry eye–related tear film impairment.[26] After adding 5 μL of 1% RB solution (330000; Sigma) to the middle of the lower eyelid, the results were recorded on a cornea diagram and graded. For grading, each cornea was considered in four quadrants, and staining scores were evaluated in each as follows: 0, without staining; 1, punctate staining; 2, continuous staining covering 50% area; 3, continuous staining covering 50% area but not confluent; and 4, confluent staining.

Histochemical and Immunohistochemical Staining

The LGs were fixed in 10% formalin for 24 hours and dehydrated in ethanol (50%, 70%, 80%, 90%, and 100%) for 30 seconds. LGs were then washed in xylene and embedded in paraffin to make sections (7 μm thick). Immunohistochemical staining was performed by incubating LG sections with goat anti-CD45 antibody (ab10558; Abcam, Cambridge, MA) overnight at 4°C; then, sections were incubated with secondary antibodies and visualized using an AEC detection kit (AEC-0038; MXB, Fujian, China), according to the manufacturer's instructions. The images were captured using a light microscope (Nikon, Tokyo, Japan). For hematoxylin and eosin staining, LG sections were stained with hematoxylin and eosin, and images were captured with a microscope (Nikon). Acinar cell areas were analyzed by using ImageJ software version 1.53a (NIH, Bethesda, MD; *http://imagej.nih.gov/ij*) after obtaining three random histologic areas of each section from the LG tissue of each mouse. Each group consisted of three mice.

Real-Time PCR

The total RNA of the cornea, LG, and meibomian gland (MG) was isolated by using the TransZol Up Plus RNA kit (ER501-01; TransGen Biotech, Beijing, China). cDNA was synthesized with HiScript III RT SuperMix (R323-01; Vazyme, Nanjing, China). The PCR primers are shown in Table 1. Real-time PCR was performed using ChamQ Universal SYBR qPCR Master Mix (Q711-02; Vazyme). Relative gene expression was calculated using the comparative Δ cycle threshold (C_T) method that involves C_T values of a housekeeping gene and β-actin mRNA levels normalized to control levels.

Table 1 Mouse Primer Sequences Used for Real-Time PCR

Primer name	Primer sequence
IL-6	F:5′-ACCACTCCCAACAGACCTGTCT-3′
	R:5′-CAGATTGTTTTCTGCAAGTGCAT-3′
IL-10	F:5′-CAGAGAAGCATGGCCCAGAA-3′
	R:5′-CACCTTGGTCTTGGAGCTTATTAAA-3′
TNF-α	F:5′-ACAAGGCTGCCCCGACTAC-3′
	R:5′-TGGGCTCATACCAGGGTTTG-3′
TH	F:5′-GGCTTCTCTGACCAGGCGTAT-3′
	R:5′-TGCTTGTATTGGAAGGCAATCTC-3′
NeT	F:5′-AACTTCAAGCCGCTCACCTA-3′
	R:5′-ATGACATAGGCAGGGACCAG-3′
VMAT2	F:5′-CGAGTGCAGCCAGAAAGTCA-3′
	R:5′-CATGGTCTCCATCATCCAGATG-3′
β-Actin	F:5′-ACGGCCAGGTCATCACTATTG-3′
	R:5′-AGAGGTCTTTACGGATGTCAACGT-3′
Elovl3	F:5′-TGGACCTGATGCAACCCTATG-3′
	R:5′-TGAAGCTCTTCCGCGTTCTC-3′
SOAT1	F:5′-AGCAAGATGAAGCCCAGAAAAA-3′
	R:5′-CATCGAAGTGGCACCCAACT-3′
DHCR24	F:5′-GCTGCGAGTCGGAAAGTACAA-3′
	R:5′-CAGCCAATGGAGTTCAGCAA-3′
HMGCR	F:5′-AAAATAAACCAAACCCCGTAACC-3′
	R:5′-CTTCGTCCAGACCCAAGGAA-3′
Nrf2	F:5′-AGGCCCAGTCCCTCAATAGC-3′
	R:5′-CGGTAGTATCAGCCAGCTGCTT-3′
HO-1	F:5′-CACAGATGGCGTCACTTCGT-3′
	R:5′-TTGCCAACAGGAAGCTGAGA-3′
Adra1a	F:5′-CTGCCATTCTTCCTCGTGAT-3′
	R:5′-GCTTGGAAGACTGCCTTCTG-3′
Adra1b	F:5′-CGGACGCCAACCAACTACTT-3′
	R:5′-AACACAGGACATCAACCGCTG-3′
Adra1d	F:5′-GGGACCGCTACTAGGTTGGAA-3′
	R:5′-ACATACACGCGGCAGTACATG-3′
Adra2a	F:5′-GTGACACTGACGCTGGTTTG-3′
	R:5′-CCAGTAACCCATAACCTCGTTG-3′
Adra2b	F:5′-CCCTGCCTCATCATGATTCT-3′
	R:5′-GTCCATTAGCCTCTCCGACA-3′
Adra2c	F:5′-TCATCGTTTTCACCGTGGTA-3′
	R:5′-GCTCATTGGCCAGAGAAAAG-3′
Adrb1	F:5′-CTCATCGTGGTGGGTAACGTG-3′
	R:5′-ACACACAGCACATCTACCGAA-3′
Adrb2	F:5′-GGGAACGACAGCGACTTCTT-3′
	R:5′-GCCAGGACGATAACCGACAT-3′
Adrb3	F:5′-GGCCCTCTCTAGTTCCCAG-3′
	R:5′-TAGCCATCAAACCTGTTGAGC-3′

Adra, adrenoceptor alpha; Adrb, adrenoceptor beta; DHCR24, 24-dehydrocholesterol reductase; Elovl3, ELOVL fatty acid elongase 3; F, forward; HMGCR, 3-hydroxy-3-methylglutaryl-CoA reductase; HO-1, heme oxygenase-1; NeT, norepinephrine transporter; Nrf2, nuclear factor erythroid 2–related factor 2; R, reverse; SOAT1, sterol O-acyltransferase 1; TH, tyrosine hydroxylase; TNF-α, tumor necrosis factor-α; VMAT2, vesicular monoamine transporter-2.

Norepinephrine and Acetylcholine Analysis

To assess NE content in LGs, the LGs were homogenized and sonicated in assay buffer (0.01 N HCl, 1 mmol/L EDTA, and 4 mmol/L sodium metabisulfite), and cell debris was pelleted by centrifugation at 12,000 × *g* for 10 minutes at 4°C to take the supernatant. The concentration of NE in LGs was detected by an NE enzyme-linked immunosorbent assay kit (KA3836; Abnova, Taiwan, China), and the concentration

was determined according to the manufacturer's instructions. The acetylcholine level in LGs was detected by an acetylcholine enzyme-linked immunosorbent assay kit (CEA912Ge; Cloud-Clone Corp., Wuhan, China). LGs were homogenized using phosphate-buffered saline (PBS) buffer and were centrifuged at 12,000 × *g* for 10 minutes at 4°C to remove debris. Acetylcholine levels were measured in the supernatant by following the manufacturer's instructions. All tissue samples were normalized to total tissue protein concentration and determined using the BCA Protein Assay kit (P0012; Beyotime, Shanghai, China), according to the manufacturer's instructions.

Western Blot Analysis

The total protein of LGs was extracted by using radioimmunoprecipitation assay buffer (Beyotime), and the protein samples were separated on SDS polyacrylamide gels and transferred to polyvinylidene difluoride membranes (Millipore, Billerica, MA). After blocking in 5% bovine serum albumin for 1 hour, the blots were incubated with rabbit anti−tyrosine hydroxylase (TH; AB152; Millipore) or anti−choline acetyltransferase (ab178850; Abcam) overnight at 4°C, and incubated with horseradish peroxidase−conjugated goat anti-rabbit secondary antibody (SA00001-2; Proteintech, Wuhan, China) or horseradish peroxidase−conjugated anti−β-actin antibody (HRP-60008; Proteintech) for 1 hour at room temperature. The blots were then visualized by enzyme-linked chemiluminescence using the electrochemiluminescence kit (Millipore) and CD-touch (Bio-Rad, Hercules, CA). Finally, the image intensity was calculated with Image Lab 5.2.1 software (Bio-Rad).

Immunofluorescence Staining

For immunofluorescence staining, LGs, MGs, eyes, and adnexa were embedded in TissueTek OCT compound (Sakura, Torrance, CA) and cut into sections (7 μm thick) using a microtome. Sections were fixed in 4% paraformaldehyde at room temperature for 10 minutes and then washed three times with PBS for 5 minutes each. The sections were permeabilized with 0.2% Triton for 5 minutes. The tissue sections were then blocked with 10% normal horse serum for 1 hour at room temperature and incubated with the following primary antibodies overnight at 4°C: mouse anti-TH antibody (MAB7566; RD, Minneapolis, MN), rabbit anti−Fos proto-oncogene positive (c-FOS) antibody (ab222699; Abcam), rabbit anti−peroxisome proliferator-activated receptor (PPAR)-γ antibody (ab45036; Abcam), and rabbit anti-mucin 1 (Muc1) antibody (ab45167; Abcam). Subsequently, the sections were incubated with fluorescein-conjugated secondary antibody for 2 hours at room temperature: Alexa 488 or 594 labeled goat anti-mouse IgG or goat anti-rabbit IgG (Invitrogen, Waltham, MA). After washing with PBS, the sections were incubated with DAPI for 5 minutes to stain the cell nuclei. The tissues were imaged with a fluorescence microscope (Zeiss, Oberkochen, Germany).

Oil Red O Staining

The frozen sections of the MGs were fixed in 4% paraformaldehyde for 10 minutes and washed in PBS for 5 minutes, and then stained for 10 minutes in freshly prepared oil red O solution. Sections were washed in PBS for 5 minutes, counterstained with hematoxylin, and mounted in 90% glycerol. Images were captured with a microscope (Nikon).

Periodic Acid−Schiff Staining

The paraffin sections of the eyes and adnexa were stained by using a periodic acid−Schiff staining kit (MST-8038; MXB, Fuzhou, China) following the manufacturer's instructions. The stained sections were then imaged using a virtual microscope (Nikon). The number of goblet cells filled with conjunctival mucin was counted from six eyes in each group.

Mitochondrial Respiration Analysis

The Seahorse XFp Flux Analyzer and XF Cell Mito Stress Test Kit (Seahorse Bioscience, Billerica, MA) were used to measure the metabolic profiles of the LG. The oxygen consumption rate was determined using the Seahorse XFp Flux Analyzer. Key parameters of mitochondrial respiratory function were measured by using a Seahorse XF Cell Mito Stress Test Kit, as described previously.[26]

mtDNA Copy Number Analysis

Total DNA was extracted from the LGs by using the EasyPure Genomic DNA Kit (EE101-11; TransGen Biotech, Beijing, China). mtDNA copy number was measured by PCR using primers for cytochrome c oxidase I (COX1), NADH dehydrogenase (ND)1, ND6, and β-globin (Hbb-b1) (Table 2). HBB1 was selected as an internal reference gene in nuclear DNA analysis. The mtDNA copy number was calculated as the ratio of mtDNA/nuclear DNA.[26,27]

Measurement of Mitochondrial and Cytosolic GSH

Mitochondrial and cytosolic proteins were isolated from the LGs by using a Tissue Mitochondria Isolation Kit (C3606; Beyotime). During centrifugation, the supernatant was collected as the cytosol portion, whereas the mitochondrial pellet was lysed in a mitochondria-specific buffer. The GSH content of the harvested samples was immediately analyzed. Mitochondrial and cytosolic GSH was measured using a Total Glutathione Assay kit (S0052; Beyotime) following the manufacturer's protocol.

Table 2 Primer Sequences Used in Mitochondrial DNA Copy Number Analysis

Primer name	Primer sequence
Hbb-b1	F:5′-GGACCCAGCGGTACTTTGATAG-3′
	R:5′-TGGCAAAGGTGCCCTTGA-3′
COX1	F:5′-GGACCCAATTCTCTACCAGCAT-3′
	R:5′-TGCTCATACTATTCCTATATAGCCGAAA-3′
ND1	F:5′-CCCTACCAATACCACACCCATT-3′
	R:5′-GGGCTACGGCTCGTAAGCT-3′
ND6	F:5′-CATACATCAACCAATCTCCCAAAC-3′
	R:5′-GACTGCTATAGCTACTGAGGAATATCCA-3′

COX1, cytochrome c oxidase I; F, forward; Hbb-b1, β-globin; ND, NADH dehydrogenase; R, reverse.

Dihydroethidium Staining

Freshly prepared LG frozen slices were incubated with 3 μmol/L dihydroethidium (S0063; Beyotime) in a humidified chamber and protected from light in a 37°C incubator for 30 minutes. The sections were then incubated with DAPI for 5 minutes. Labeling was imaged with a fluorescence microscope (Zeiss). The fluorescence intensity was calculated using ImageJ software version 1.53a.

Electron Microscopy Analysis

After the indicated treatment, LGs were cut into 1-mm^3 blocks and first fixed in 2.5% prechilled glutaraldehyde. The samples were then examined using a JEM-1200EX transmission electron microscope (JEOL, Tokyo, Japan). ImageJ software version 1.53a was used to measure the mitochondrial size and mitochondrial density.

Statistical Analysis

All data were generated from at least three independent experiments. Statistical analyses were performed with GraphPad Prism 8 software (GraphPad Software, San Diego, CA) and SPSS19.0 software (SPSS Inc., Chicago, IL). All data were expressed as means ± SD. Statistical analysis was performed using the unpaired *t*-test and one-way analysis of variance. Values were considered statistically significant if $P < 0.05$.

Results

Hyperglycemia Causes Tear Reduction and Dry Eye in Diabetic Mice

To determine the characteristics of dry eye in chronic hyperglycemic conditions, an STZ-induced model of type 1 DM mice was established. Mice were observed at regular time points of 0, 2, 4, 8, and 16 weeks after STZ i.p. injection. Compared with the control group, the blood glucose level in the DM group was much higher within 2 weeks, and the body weight of the DM group showed a gradual decrease over 2 weeks (Supplemental Figure S1), indicating a successful animal model of DM. Meanwhile, tear production decreased to 62%, 44%, 36%, and 34% at 2, 4, 8, and 16 weeks, respectively, in diabetic mice compared with normal mice (Figure 1A). Subsequently, corneal RB staining was performed to detect the corneal epithelium defect. There were no statistical differences during 0 and 4 weeks; however, at 8 and 16 weeks, the RB score increased by 1.6-fold and 3.3-fold compared with the control group (Figure 1, B and C). In addition, because hyperglycemia caused by type 1 DM can lead to a systemic inflammatory response,[28,29] inflammatory infiltration of the cornea and LG was evaluated. As shown in Figure 1, D and F, the real-time PCR arrays indicated that proinflammatory factors tumor necrosis factor-α and IL-6 were significantly increased and anti-inflammatory cytokine IL-10 was markedly decreased. In addition, positive staining of CD45 (a pan-leukocyte marker) was detected in LG of diabetic mice (Figure 1E). Likewise, hematoxylin and eosin staining showed that the LG acinar cell area ratio was significantly reduced in diabetic mice, accompanied by a significant increase in inflammatory cell infiltration (mainly monocytes) (Supplemental Figure S2). These findings confirmed establishment of a successful diabetic dry eye model and allowed for further investigation of the change in NE release during the progression of dry eye.

Hyperglycemia Promotes NE Release in the Lacrimal Gland

The parasympathetic cholinergic system is the principal regulator of LG protein and fluid secretion.[11] First, the study measured parasympathetic nerve activity in response to hyperglycemia. The content of acetylcholine, a parasympathetic neurotransmitter, was highly reduced in the LG of diabetic mice. This was accompanied by the down-regulation of choline acetyltransferase, an enzyme responsible for acetylcholine synthesis (Supplemental Figure S3). These data were consistent with previous findings that blocking the parasympathetic stimulation of LG contributes to the loss of tear-secreting ability.[18] Next, the study explored the involvement of the sympathetic neurotransmitter NE in diabetic dry eye. Interestingly, NE levels were elevated in diabetic LGs, indicating sympathetic activation (Figure 2A). The expression of noradrenergic markers was measured to further verify the enhanced NE release.[30] Hyperglycemia caused the induction of TH, norepinephrine transporter, and vesicular monoamine transporter-2 (Figure 2B). Similarly, TH protein expression levels in diabetic LGs were much higher than in normal controls (Figure 2, C and D). Because the LG sympathetic nerve originates from the SCG,[31] whether increased NE production in the LG was accompanied by neuronal activation of the SCG was explored next. c-FOS, a marker of neuronal activation in SCG neurons, was immunostained and

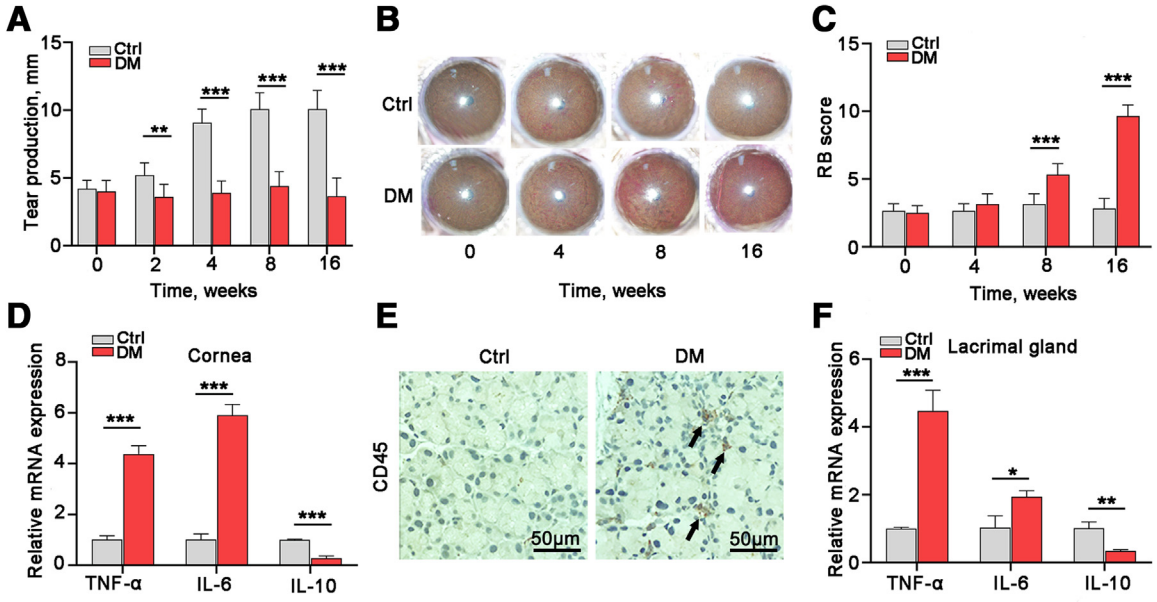

Figure 1 Diabetes mellitus (DM)—impaired tear production and dry eye onset in mice. **A:** Tear production of control (Ctrl) and diabetic mice at 0, 2, 4, 8, and 16 weeks after streptozotocin (STZ) injection. **B** and **C:** Corneal Rose Bengal (RB) staining and score of Ctrl and DM mice after 0, 4, 8, and 16 weeks of i.p. STZ injection. **D:** Comparisons of the expressions of the inflammatory cytokine tumor necrosis factor-α (TNF-α), IL-6, and IL-10 mRNA in the corneas at 16 weeks of DM mice and age-matched Ctrl mice. **E:** Immunohistochemical staining of CD45 in lacrimal glands (LGs) at 16 weeks of DM mice and age-matched Ctrl mice. **Arrows** indicate positive staining. **F:** Comparisons of the expressions of inflammatory cytokine TNF-α, IL-6, and IL-10 mRNA in the LGs at 16 weeks of DM mice and age-matched Ctrl mice. Data are shown as means ± SD (**A**, **C**, **D**, and **F**). $n = 3$ to 10 mice per group (**A**–**F**). $^{*}P < 0.05$, $^{**}P < 0.01$, and $^{***}P < 0.001$. Scale bars = 50 μm (**E**).

analyzed. A significant increase in immunoreactivity for c-FOS in SCG cells was observed in diabetic mice compared with their controls (Figure 2, E and F). Collectively, the present findings indicated that reduced tear secretion in diabetic mice was not determined merely by parasympathetic activity but by the involvement of the sympathetic nervous system.

Surgical and Chemical Sympathectomy Ameliorates Tear Reduction and Diabetic Dry Eye

To test whether NE was responsible for dry eye in diabetic mice, two strategies to reduce the source of LG NE in diabetic mice were tested: chemical denervation using 6-OHDA, a selective neurotoxin for peripheral sympathetic nerves; and physical denervation by SCGx (Figure 3A). A marked reduction of NE in LG was observed in the 6-OHDA and SCGx treatment groups compared with diabetic mice (0.59 ± 0.11 versus 0.04 ± 0.01 versus 0.05 ± 0.01 ng/mg) (Figure 3B). TH protein expression levels in LG were much lower compared with the diabetic group (Supplemental Figure S4, A and B), and a significant decrease in SCG cells immunoreactive for c-FOS was observed in the treatment group compared with the diabetic group (Supplemental Figure S4, C and D).

The effects of 6-OHDA and SCGx treatment on dry eye at 16 weeks were investigated in diabetic mice. Treatment with 6-OHDA and SCGx was protective in the diabetic model, as shown in Figure 3C, with tear production increasing 1.75-fold and 1.7-fold, respectively, compared with the diabetic group after 7 days of treatment. In addition, denervation of the sympathetic nervous system improved the corneal epithelium defect and response to inflammation (Figure 3, D–F). For LGs, weaker immunostaining for CD45 and attenuated obvious inflammation were observed after blocking the source of NE (Figure 3, G and H). Together, these data indicated that the reduction in the NE content in the LG of diabetic mice could relieve tear secretion and symptoms of diabetic dry eye, such as ocular epithelium defect and LG inflammation.

α_1AR Antagonist Improves Tear Reduction and Dry Eye in Diabetic Mice

Because NE binds to the ARs and mediates a cascade of cellular responses,[21] AR expression was studied in the LGs of mice. Real-time PCR results showed that mice LGs expressed a large amount of α_{1A}, α_{1D}, β_1, and β_2AR (Figure 4A). After i.p. injection of prazosin (an α_1AR antagonist) and propranolol (a βAR antagonist) in diabetic mice, the blockade of α_1AR resulted in increased tear secretion, whereas blockade of βAR did not affect tear secretion (Figure 4B). Subsequently, a series of clinically selective oral α_1AR antagonists were used in diabetic mice, including prazosin, alfuzosin, terazosin, and doxazosin,[24] to determine the effect of α_1AR antagonists. As shown in Figure 4C, all types of α_1AR antagonists increased tear

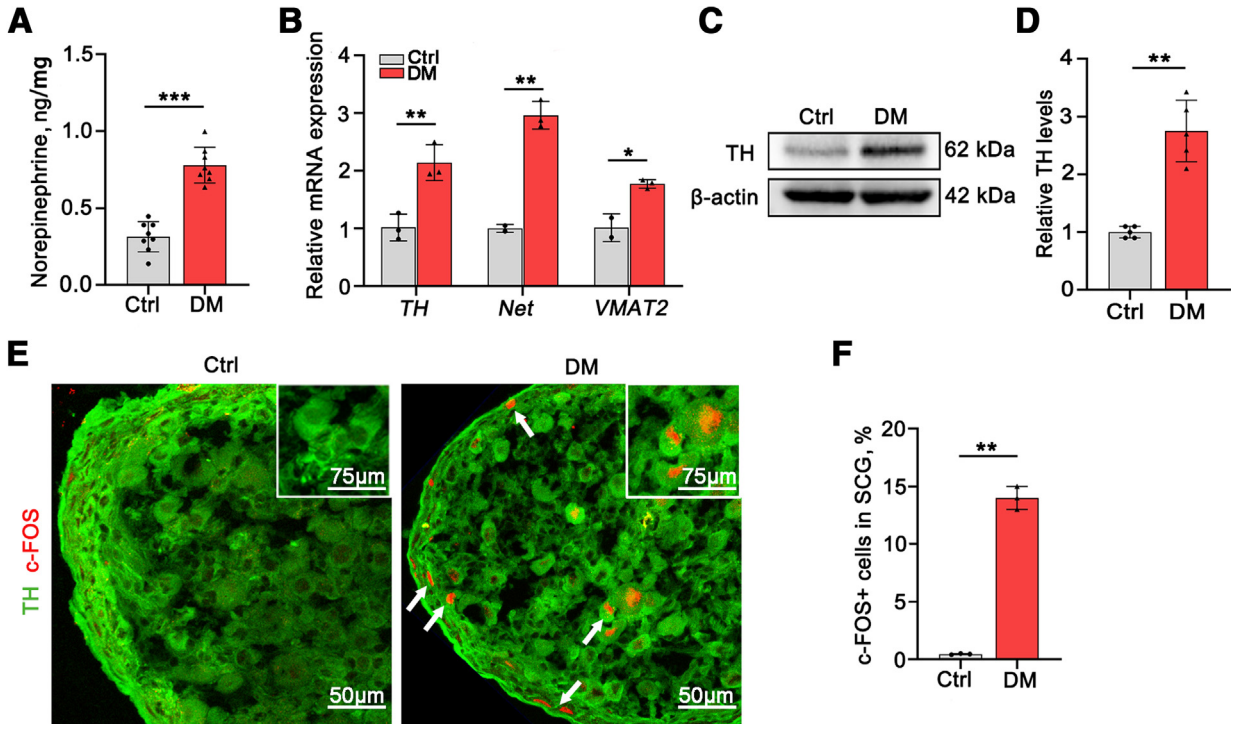

Figure 2 Sympatho-adrenergic activation of the lacrimal gland (LG) in diabetic mice. **A:** Enzyme-linked immunosorbent assay of LG norepinephrine concentrations in control (Ctrl) mice and mice with diabetes mellitus (DM). **B:** Comparisons of the mRNA expressions of tyrosine hydroxylase (TH), norepinephrine transporter (NeT), and vesicular monoamine transporter-2 (VMAT2) in LGs of Ctrl and DM mice. **C:** Western blot analysis to detect TH in LGs of Ctrl and DM mice. **D:** Quantification of the TH protein in LGs of Ctrl and DM mice. **E:** Immunofluorescence staining of the superior cervical ganglion (SCG) for TH (green) and Fos proto-oncogene (c-FOS; red) of Ctrl and DM mice. **White arrows** point to positive staining. **Insets:** Highly magnified sections. **F:** Quantification of c-FOS$^+$ cells in SCG of Ctrl and DM mice. Data are shown as means ± SD (**A**, **B**, **D**, and **F**). n = 3 to 8 mice per group (**A**–**F**).*$P < 0.05$, **$P < 0.01$, and ***$P < 0.001$. Scale bars: 50 μm (**E**, **main images**); 75 μm (**E**, **insets**).

secretion, whereas the effect of alfuzosin on increasing tear production was more stable.

Corneal RB staining and the RB score were significantly reduced after 7 days of alfuzosin treatment compared with untreated diabetic eyes (Figure 4, D and E). Alfuzosin treatment suppressed corneal tumor necrosis factor-α and IL-6 expression and increased IL-10 expression (Figure 4F). Immunofluorescence staining and real-time PCR were used to detect the expression of LG inflammation. As shown in Figure 4G, the immunostaining for CD45 immune cells decreased after alfuzosin treatment. Lower mRNA levels of proinflammatory genes tumor necrosis factor-α and IL-6, and higher mRNA levels of anti-inflammatory factor gene IL-10, were found after alfuzosin treatment (Figure 4H). Therefore, these data indicated that α_1AR played the predominant role in the regulation of tear production in LG, and α_1AR antagonist could increase tear secretion, reduce LG inflammation, and reduce ocular surface damage in diabetic mice.

Targeted Inhibition of α_1AR Alleviates the Dysfunction of Diabetic Ocular Surface

Tear components were secreted from the LG, MG, corneal epithelium, and conjunctival epithelium in humans.[32] Whether the physiological functions of MG and the conjunctiva were affected by alfuzosin in diabetic mice was studied next.

Meibomian lipids synthesized by acini are essential to maintaining the integrity and health of the ocular surface.[33] Lipid metabolism disorder is one of the most common characteristics of meibomian gland dysfunction.[34] The oil red O staining was used to clarify the distribution of lipids in MG tissues and revealed more condensed staining in the acini of the alfuzosin-treated group than in the untreated diabetic group (Figure 5A). PPAR-γ, as the main subtype of the PPAR family, is important in cell differentiation and various metabolic processes, especially lipid and glucose homeostasis.[35] Immunofluorescence staining for PPAR-γ showed both cytoplasmic and nuclear staining, whereas alfuzosin-treated mice showed an increase in PPAR-γ fluorescence intensity (Figure 5B). Guo et al[36] have reported reduced expression of lipid synthesis–related genes in diabetic MGs. Real-time PCR revealed significantly upregulated ELOVL fatty acid elongase 3 (Elovl3), sterol O-acyltransferase 1 (SOAT1), 24-dehydrocholesterol reductase (DHCR24), and 3-hydroxy-3-methylglutaryl-CoA reductase (HMGCR) mRNA expression after alfuzosin treatment in diabetic MG (Figure 5C).

Periodic acid–Schiff staining indicated that the number of conjunctival goblet cells was significantly increased by twofold (15.79 ± 4.11 versus 30.01 ± 9.61 cells/100 μm)

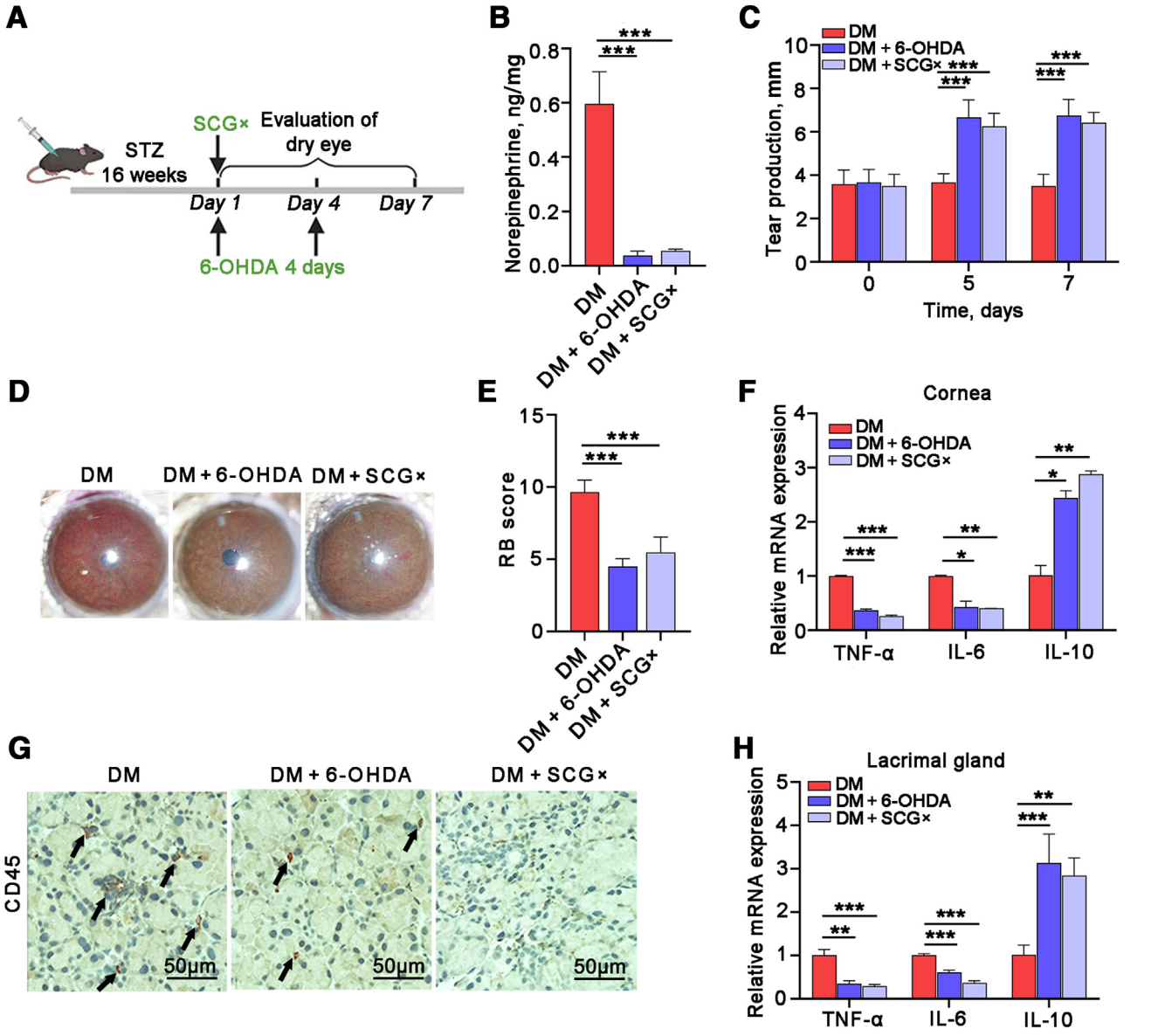

Figure 3 Effects of norepinephrine (NE) elimination on tear production and diabetic dry eye. **A:** Diabetic mice were subjected to different models of sympathetic neuronal ablation. 6-Hydroxydopamine (6-OHDA) hydrobromide was administered intraperitoneally every day for 4 days. **B:** Effect of 6-OHDA or superior cervical ganglionectomy (SCGx) treatment on NE concentrations in lacrimal gland (LG) of mice with diabetes mellitus (DM). **C:** Tear volume production in DM mice was measured on days 5 and 7 after 6-OHDA or SCGx treatment. **D** and **E:** Corneal Rose Bengal (RB) staining and scoring were performed in DM mice treated with 6-OHDA or SCGx for 7 days. **F:** Expression of tumor necrosis factor-α (TNF-α), IL-6, and IL-10 mRNA in the cornea of DM mice treated with 6-OHDA or SCGx for 7 days. **G:** Immunohistochemical staining of $CD45^+$ cells in the LGs of DM mice treated with 6-OHDA or SCGx for 7 days. **Black arrows** point to positive staining. **H:** Quantification of the amounts of TNF-α, IL-6, and IL-10 mRNA expressed in LGs after 7 days of 6-OHDA or SCGx treatment in DM mice. Data are shown as means ± SD (**B**, **C**, **E**, **F**, and **H**). $n = 3$ to 6 mice per group (**B**–**H**). $^*P < 0.05$, $^{**}P < 0.01$, and $^{***}P < 0.001$. Scale bars = 50 μm (**G**). STZ, streptozotocin.

(Figure 5, D and E) in alfuzosin-treated groups compared with the untreated DM mouse group. Conjunctival sections were stained by immunofluorescence for Muc1, which marked mucins,[37] and the expression of Muc1 was increased in the alfuzosin treatment group compared with the untreated DM group (Figure 5F). These data suggested that alfuzosin may alleviate diabetes-related damage to the MG and conjunctiva, thus relieving dry eye associated with diabetes.

Alfuzosin Improves the Mitochondrial Bioenergetic Deficit of Diabetic Lacrimal Gland

Previous studies have shown that hyperglycemia-induced severe mitochondrial bioenergetic deficit of LG contributes to the early onset of dry eye in DM mice.[26] To evaluate the influence of alfuzosin on diabetic LGs, diabetic and alfuzosin-treated diabetic LGs were collected for the analysis of mitochondrial activity, mtDNA copy number, GSH

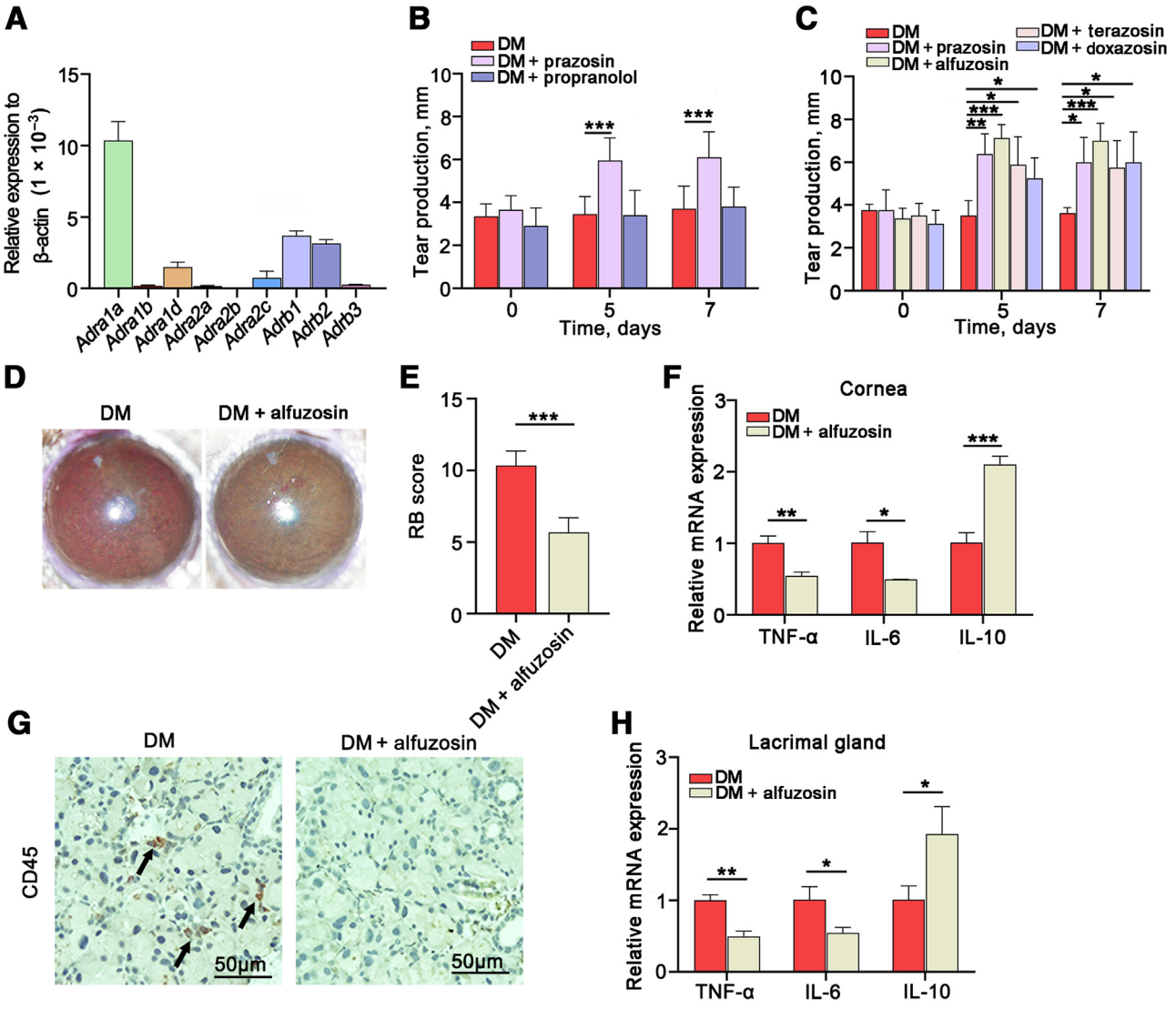

Figure 4 Regulation of α_1 adrenergic receptor (AR) antagonist in tear reduction and diabetic dry eye. **A:** Relative expression of AR mRNA in the lacrimal glands (LGs) of mice. **B:** Tear production after prazosin (an α_1AR antagonist) or propranolol (a βAR antagonist) treatment in mice with diabetes mellitus (DM). **C:** Tear production after a series of α_1AR antagonist treatment of DM mice. **D** and **E:** Changes in corneal Rose Bengal (RB) staining and score after alfuzosin treatment in DM mice. **F:** Changes in the relative expression of inflammatory factor tumor necrosis factor-α (TNF-α), IL-6, and IL-10 mRNA in the cornea after alfuzosin treatment in DM mice. **G:** Immunohistochemical staining of CD45 in LG after alfuzosin treatment in DM mice. **Black arrows** point to positive staining. **H:** Quantification of mRNA levels of the inflammatory cytokines TNF-α, IL-6, and IL-10 expressed by alfuzosin-treated LGs in DM mice. Data are shown as means ± SD (**A**–**C**, **E**, **F**, and **H**). $n = 3$ to 10 mice per group (**A**–**H**). $^*P < 0.05$, $^{**}P < 0.01$, and $^{***}P < 0.001$. Scale bars = 50 μm (**G**).

level, reactive oxygen species (ROS) level, and antioxidant factors. The oxygen consumption rate was measured by using the Seahorse XFp Analyzer. Alfuzosin-treated LG cells assumed a significant increase in basal, ATP-linked, maximal respiration and nonmitochondrial oxygen consumption, but not in proton leak or reserve capacity, compared with untreated DM mice (Figure 6, A and B). Furthermore, alfuzosin treatment alleviated enhanced mitochondrial fission and decreased mitochondrial size caused by hyperglycemia (Supplemental Figure S5). In addition, the relative numbers of mtDNA copies of COX1, ND1, and ND6 per Hbb-b1 of alfuzosin-treated LGs were increased compared with untreated DM mice (Figure 6C). Consistently, the mitochondrial glutathione level showed a 50% increase, whereas the cytosolic GSH level did not show significant change after alfuzosin treatment (Figure 6D). Oxidative stress due to ROS overproduction plays a fundamental role in diabetes.[38] Mitochondria are the main source of ROS, and the mitochondrial structure can be damaged by excessive ROS.[39] Dihydroethidium was used to detect ROS production *in situ*. ROS decreased in LGs after alfuzosin treatment (Figure 6, E and F). Moreover, the mRNA expression of major intracellular free radical scavengers, including nuclear factor erythroid 2–related factor 2

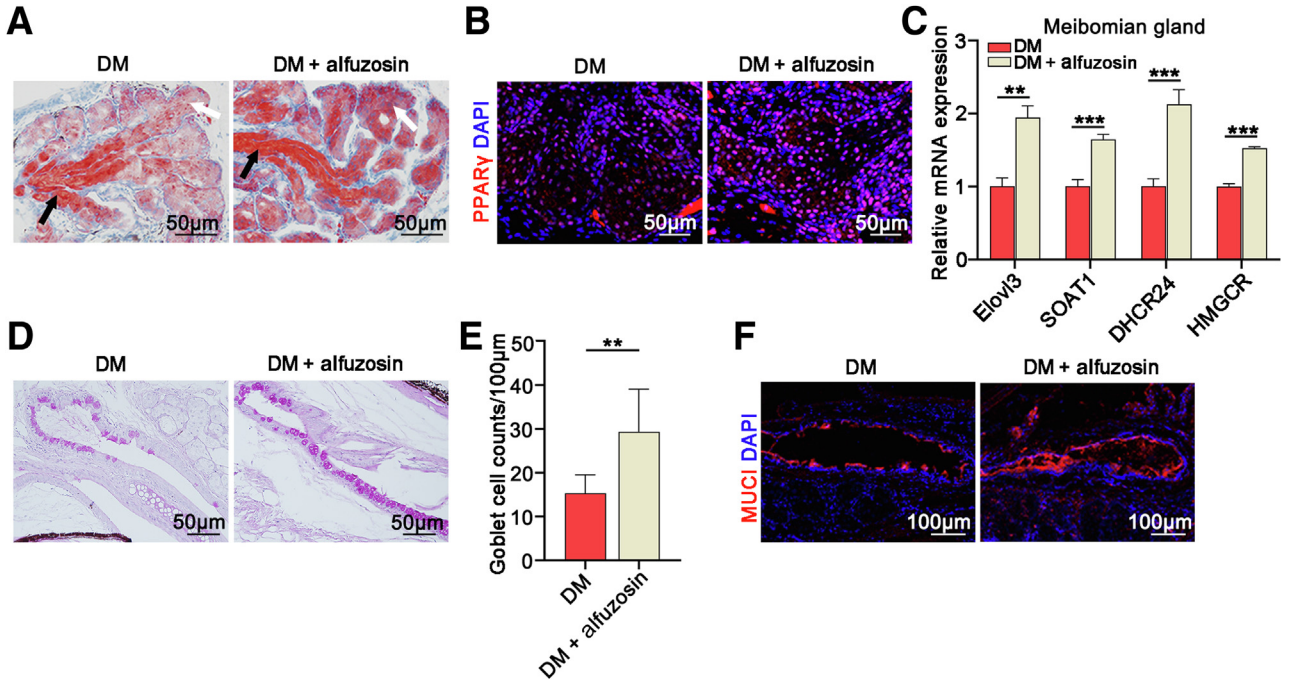

Figure 5 Influence of α_1 adrenergic receptor (AR) antagonist on diabetic meibomian gland (MG) dysfunction and conjunctival goblet cells. **A:** Oil red O staining of the MG after alfuzosin treatment or mice with diabetes mellitus (DM). **Black arrows** indicate the MG duct, and **white arrows** indicate the MG acinus. **B:** Immunofluorescence staining of peroxisome proliferator-activated receptor (PPAR)-γ in MG from alfuzosin-treated and DM mice. **C:** Relative mRNA expression of lipid metabolism—related enzymes ELOVL fatty acid elongase 3 (Elovl3), sterol O-acyltransferase 1 (SOAT1), 24-dehydrocholesterol reductase (DHCR24), and 3-hydroxy-3-methylglutaryl-CoA reductase (HMGCR) in MG of alfuzosin-treated and diabetic mice. **D** and **E:** Periodic acid—Schiff staining and goblet cell number in conjunctiva of mice in the alfuzosin treatment groups and DM groups. **F:** Immunofluorescence staining of mucin 1 (Muc1) in mice conjunctiva after alfuzosin treatment or DM mice. Data are shown as means ± SD (**C** and **E**). $n = 3$ to 6 mice per group (**A**—**F**). $^{**}P < 0.01$, $^{***}P < 0.001$. Scale bars: 50 μm (**A**, **B**, and **D**); 100 μm (**F**).

and heme oxygenase-1, was partially recovered in the diabetic LG after alfuzosin treatment (Figure 6G). These data suggest that alfuzosin might alleviate diabetic dry eye by reducing mitochondrial dysfunction and oxidative stress in diabetic LG.

Discussion

In recent years, diabetic dry eye has steadily increased in incidence and has become a significant factor in human mental and physical health.[6,7] Efforts to understand the molecular mechanisms that underlie tear reduction and dry eye have been challenging. Here, the study evaluated the release of the sympathetic neurotransmitter NE and the role of the NE-α_1AR-mitochondria axis in LGs in the pathogenesis of diabetic dry eye. Unlike previous reports showing that NE and phenylephrine (an α_1AR agonist) induce significant protein secretion from LG *in vitro*,[40–42] the study showed, for the first time, that in diabetic mice, α_1AR antagonist alfuzosin ameliorated tear reduction and dry eye severity, including corneal epithelial barrier function, lacrimal and corneal inflammation, as well as impairments of MG and density of conjunctival goblet cells. Alfuzosin exhibited a role in the mitochondrial bioenergetics of LG restoration, which is linked to mitochondrial dysfunction in the early stages of dry eye.[26] In general, this study indicated that elevated neurotransmitter NE in diabetic LG is a pathogenic factor for diabetic dry eye and suggested that modification of α_1AR activity may prevent or treat diabetic dry eye.

Chronic sympathetic activation favors the development of diabetes-related end-organ damage, including endothelial dysfunction, cardiac hypertrophy, and renal impairment.[43,44] Pharmacologic inhibition of the sympathetic nervous system is regarded as a goal in the therapeutic approach to diabetes.[45] Previous studies have shown that a series of tissues related to the ocular surface, including the LG, MG, and conjunctiva, are impaired in hyperglycemia.[26,36] Furthermore, the study innovatively demonstrated that hyperglycemia promoted sympathetic nerve activity in LG and SCG, whereas depletion of NE or blockade of NE-α_1AR pathway alleviated LG inflammation, MG dysfunction, and loss of goblet cells. More importantly, the safety and efficacy of alfuzosin have been well assessed for the treatment of male prostatic hyperplasia,[46] making alfuzosin a potential treatment for diabetic LG. Whether alfuzosin and artificial tears work synergistically, independently, or mutually exclusively in the treatment of dry eye remains elusive and deserves further investigation.

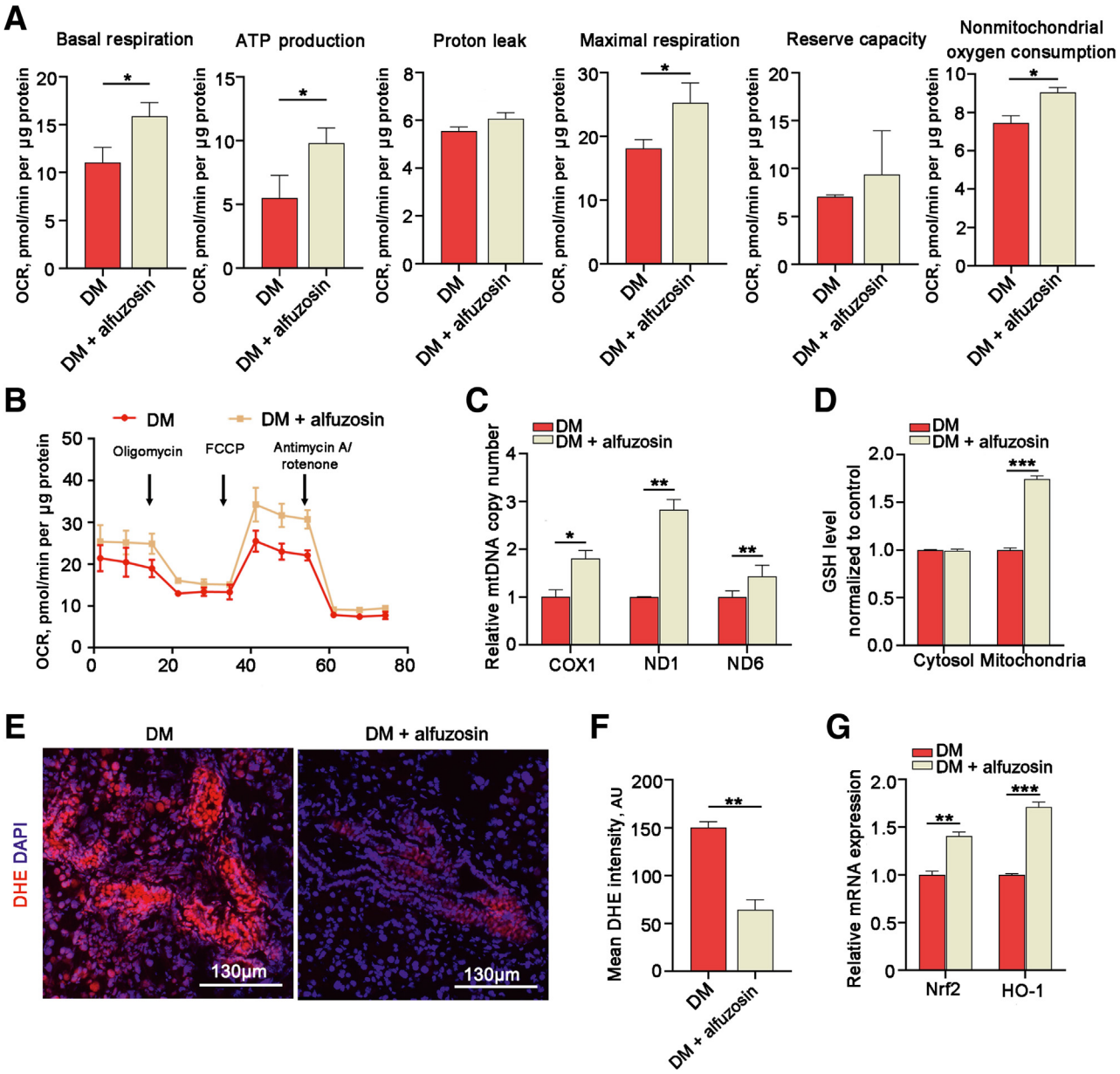

Figure 6 α_1 Adrenergic receptor (AR) antagonist repaired mitochondrial bioenergetics of diabetic lacrimal gland. **A** and **B:** Mitochondrial functions of lacrimal gland (LG) cells were evaluated with the Seahorse XFp Analyzer. After the measurement of basal oxygen consumption rate (OCR), ATP-linked respiration and proton leak were determined after oligomycin injection (1.5 µmol/L final), maximal respiration was determined after injection of trifluoromethoxy carbonylcyanide phenylhydrazone (FCCP) (0.5 µmol/L), reserve capacity was measured as the difference between maximal and basal respiration, and all parameters were calculated subtracting nonmitochondrial respiration. **C:** Relative mitochondrial DNA copy numbers of cytochrome c oxidase I (COX1), NADH dehydrogenase (ND)1, and ND6 per β-globin (Hbb-b1) in LGs of mice with diabetes mellitus (DM) treated with alfuzosin. **D:** Glutathione (GSH) levels in the cytosolic and mitochondrial pools of LG cells in DM mice treated with alfuzosin. **E** and **F:** Immunofluorescence staining of dihydroethidium (DHE) in LGs of alfuzosin-treated DM mice. **G:** Relative expression of nuclear factor erythroid 2–related factor 2 (Nrf2) and heme oxygenase-1 (HO-1) mRNA of alfuzosin-treated diabetic LGs. Data are shown as means ± SD (**A**–**D**, **F**, and **G**). $n = 3$ mice per group (**A**–**G**). $^*P < 0.05$, $^{**}P < 0.01$, and $^{***}P < 0.001$. Scale bars = 130 µm (**E**). AU, arbitrary unit.

NE released from sympathetic nerves can activate α_1, α_2, or βAR signaling pathways, depending on the target tissue. Using video microscopy, Szarka et al[47] observed that NE initiated a rapid and robust fluid secretory response in isolated mouse LG ducts which was completely blocked by α_{1D}AR antagonist BMY-7378. Similarly, Dartt and Hodges[16] found that in isolated rat LG acini, α_1AR agonist stimulated protein secretion.[48] Apart from the generally accepted decisive role of α_{1D}AR *in vitro*, little is known about the direct effect of α_1AR regulation of LG function *in vivo* and under pathologic circumstances. This study detected significantly elevated levels of NE in LG during diabetic dry eye progression. Further screening experiments demonstrated, for the first time, that selective

inhibition of the α_1AR-mediated pathway promoted tear secretion. Stimulation of the α_1AR promotes salivary secretion.[49] However, repeated administration of α_1AR agonist phenylephrine in mice causes a significant decrease in salivary protein concentration.[50] Similarly, this study showed that LG with diabetes was exposed to long-term sympathetic activation, leading to tear reduction through α_1AR. In addition, it compared the expression of AR genes in LG. Real-time PCR array was used to show that the expression of α_{1A}AR was the highest, followed by βAR and α_{1D}AR. This finding provides novel information on the role of α_{1A}AR in LG function.

Mitochondrial energy has been proposed as a mechanism underlying the action of alfuzosin, because mitochondrial dysfunction is a common mechanism of diabetic complications.[51,52] Tight regulation of mitochondrial activity is critical for glandular tissue homeostasis, including the pancreas, salivary glands, and mammary glands.[53–55] *In vivo* and *in vitro* studies have demonstrated that ROS overproduction and oxidative stress are potential mechanisms of dry eye disease.[56,57] Oxidative stress causes mitochondrial damage, which affects mitochondrial function. As such, alterations in mitochondrial structure and mitochondrial function are associated with metabolic disorders in which oxidative stress appears to be a key factor.[58] In addition, severe mitochondrial dysfunction of the LGs may lead to the early onset of diabetic dry eye, and topical application of mitochondria-targeted antioxidants SkQ1 and SS31 attenuated the severity of diabetic dry eye.[26] It is suggested that alleviating mitochondrial dysfunction provides a new strategy for the treatment of dry eye disease. The current findings indicated that alfuzosin has a significant restorative effect on mitochondrial function and deepened our understanding of the role of the NE-α_1AR-mitochondria axis in general homeostasis. Further insight into the impact of alfuzosin on cell functions in LGs may inform the development of improved treatments for diabetes dry eye.

Collectively, the study demonstrates the influence of the NE-α_1AR-mitochondria axis on the development of the dry eye in the type 1 DM mouse model. In the future, diabetic dry eye might be alleviated by blocking the source of NE and α_1AR antagonism, and the present findings might lead to further novel treatment strategies.

Author Contributions

S.Z. performed experiments, interpreted the data, and wrote and revised the manuscript; Q.W. and M.Q. analyzed data and wrote the manuscript; Q.C., X.B., and Z.Z. performed animal experiments; and L.X. and Q.Z. designed the study, managed funding, and supervised the work. All authors read and agreed on the final version of the article to be submitted and published.

Supplemental Data

Supplemental material for this article can be found at *http://doi.org/10.1016/j.ajpath.2023.03.015*.

References

1. Tomic D, Shaw JE, Magliano DJ: The burden and risks of emerging complications of diabetes mellitus. Nat Rev Endocrinol 2022, 18: 525–539
2. Sun H, Saeedi P, Karuranga S, Pinkepank M, Ogurtsova K, Duncan BB, Stein C, Basit A, Chan J, Mbanya JC, Pavkov ME, Ramachandaran A, Wild SH, James S, Herman WH, Zhang P, Bommer C, Kuo S, Boyko EJ, Magliano DJ: IDF diabetes atlas: global, regional and country-level diabetes prevalence estimates for 2021 and projections for 2045. Diabetes Res Clin Pract 2022, 183:109119
3. Melendez-Ramirez LY, Richards RJ, Cefalu WT: Complications of type 1 diabetes. Endocrinol Metab Clin North Am 2010, 39:625–640
4. Yang J, Zhang LJ, Wang F, Hong T, Liu Z: Molecular imaging of diabetes and diabetic complications: beyond pancreatic β-cell targeting. Adv Drug Deliv Rev 2019, 139:32–50
5. Cole JB, Florez JC: Genetics of diabetes mellitus and diabetes complications. Nat Rev Nephrol 2020, 16:377–390
6. Manaviat MR, Rashidi M, Afkhami-Ardekani M, Shoja MR: Prevalence of dry eye syndrome and diabetic retinopathy in type 2 diabetic patients. BMC Ophthalmol 2008, 8:10
7. Achtsidis V, Eleftheriadou I, Kozanidou E, Voumvourakis KI, Stamboulis E, Theodosiadis PG, Tentolouris N: Dry eye syndrome in subjects with diabetes and association with neuropathy. Diabetes Care 2014, 37:e210–e211
8. Zou X, Lu L, Xu Y, Zhu J, He J, Zhang B, Zou H: Prevalence and clinical characteristics of dry eye disease in community-based type 2 diabetic patients: the Beixinjing eye study. BMC Ophthalmol 2018, 18:117
9. Montés-Micó R, Cerviño A, Ferrer-Blasco T, García-Lázaro S, Madrid-Costa D: The tear film and the optical quality of the eye. Ocul Surf 2010, 8:185–192
10. Veernala I, Jaffet J, Fried J, Mertsch S, Schrader S, Basu S, Vemuganti GK, Singh V: Lacrimal gland regeneration: the unmet challenges and promise for dry eye therapy. Ocul Surf 2022, 25: 129–141
11. Dartt DA: Neural regulation of lacrimal gland secretory processes: relevance in dry eye diseases. Prog Retin Eye Res 2009, 28: 155–177
12. Ruskell GL: The distribution of autonomic post-ganglionic nerve fibres to the lacrimal gland in monkeys. J Anat 1971, 109:229–242
13. Dartt DA: Dysfunctional neural regulation of lacrimal gland secretion and its role in the pathogenesis of dry eye syndromes. Ocul Surf 2004, 2:76–91
14. Nakamura S, Imada T, Jin K, Shibuya M, Sakaguchi H, Izumiseki F, Tanaka KF, Mimura M, Nishimori K, Kambara N, Hirayama N, Kamimura I, Nomoto K, Mogi K, Kikusui T, Mukai Y, Yamanaka A, Tsubota K: The oxytocin system regulates tearing. bioRxiv 2022, [Preprint] https://doi.org/10.1101/2022.03.08.483433
15. Tangkrisanavinont V: Stimulation of lacrimal secretion by sympathetic nerve impulses in the rabbit. Life Sci 1984, 34:2365–2371
16. Dartt DA, Hodges RR: Interaction of alpha1D-adrenergic and P2X(7) receptors in the rat lacrimal gland and the effect on intracellular [Ca2+] and protein secretion. Invest Ophthalmol Vis Sci 2011, 52: 5720–5729
17. Meneray MA, Bennett DJ, Nguyen DH, Beuerman RW: Effect of sensory denervation on the structure and physiologic responsiveness of rabbit lacrimal gland. Cornea 1998, 17:99–107

18. Jin K, Imada T, Hisamura R, Ito M, Toriumi H, Tanaka KF, Nakamura S, Tsubota K: Identification of lacrimal gland postganglionic innervation and its regulation of tear secretion. Am J Pathol 2020, 190:1068−1079
19. Seals DR, Bell C: Chronic sympathetic activation: consequence and cause of age-associated obesity. Diabetes 2004, 53:276−284
20. Thorp AA, Schlaich MP: Relevance of sympathetic nervous system activation in obesity and metabolic syndrome. J Diabetes Res 2015, 2015:341583
21. Vasamsetti SB, Florentin J, Coppin E, Stiekema L, Zheng KH, Nisar MU, Sembrat J, Levinthal DJ, Rojas M, Stroes E, Kim K, Dutta P: Sympathetic neuronal activation triggers myeloid progenitor proliferation and differentiation. Immunity 2018, 49:93−106.e7
22. Christoffersson G, Ratliff SS, von Herrath MG: Interference with pancreatic sympathetic signaling halts the onset of diabetes in mice. Sci Adv 2020, 6:eabb2878
23. Tóth IE, Boldogkoi Z, Medveczky I, Palkovits M: Lacrimal preganglionic neurons form a subdivision of the superior salivatory nucleus of rat: transneuronal labelling by pseudorabies virus. J Auton Nerv Syst 1999, 77:45−54
24. Masumori N: Naftopidil for the treatment of urinary symptoms in patients with benign prostatic hyperplasia. Ther Clin Risk Manag 2011, 7:227−238
25. Rosenblit PD: Common medications used by patients with type 2 diabetes mellitus: what are their effects on the lipid profile. Cardiovasc Diabetol 2016, 15:95
26. Qu M, Wan L, Dong M, Wang Y, Xie L, Zhou Q: Hyperglycemia-induced severe mitochondrial bioenergetic deficit of lacrimal gland contributes to the early onset of dry eye in diabetic mice. Free Radic Biol Med 2021, 166:313−323
27. Der Vartanian A, Quétin M, Michineau S, Auradé F, Hayashi S, Dubois C, Rocancourt D, Drayton-Libotte B, Szegedi A, Buckingham M, Conway SJ, Gervais M, Relaix F: PAX3 confers functional heterogeneity in skeletal muscle stem cell responses to environmental stress. Cell Stem Cell 2019, 24:958−973.e9
28. Elshaer SL, Alwhaibi A, Mohamed R, Lemtalsi T, Coucha M, Longo FM, El-Remessy AB: Modulation of the p75 neurotrophin receptor using LM11A-31 prevents diabetes-induced retinal vascular permeability in mice via inhibition of inflammation and the RhoA kinase pathway. Diabetologia 2019, 62:1488−1500
29. Li YJ, Chen X, Kwan TK, Loh YW, Singer J, Liu Y, Ma J, Tan J, Macia L, Mackay CR, Chadban SJ, Wu H: Dietary fiber protects against diabetic nephropathy through short-chain fatty acid-mediated activation of G protein-coupled receptors GPR43 and GPR109A. J Am Soc Nephrol 2020, 31:1267−1281
30. Gadomski S, Fielding C, García-García A, Korn C, Kapeni C, Ashraf S, Villadiego J, Toro RD, Domingues O, Skepper JN, Michel T, Zimmer J, Sendtner R, Dillon S, Poole K, Holdsworth G, Sendtner M, Toledo-Aral JJ, De Bari C, McCaskie AW, Robey PG, Méndez-Ferrer S: A cholinergic neuroskeletal interface promotes bone formation during postnatal growth and exercise. Cell Stem Cell 2022, 29:528−544.e9
31. Marchioni D, Bettini M, Soloperto D: Anatomy of the lacrimal drainage system. Endoscopic Surgery of the Lacrimal Drainage System. Edited by Presutti L, Mattioli F. Cham, Switzerland: Springer, 2016
32. Nakamachi T, Ohtaki H, Seki T, Yofu S, Kagami N, Hashimoto H, Shintani N, Baba A, Mark L, Lanekoff I, Kiss P, Farkas J, Reglodi D, Shioda S: PACAP suppresses dry eye signs by stimulating tear secretion. Nat Commun 2016, 7:12034
33. Nelson JD, Shimazaki J, Benitez-del-Castillo JM, Craig JP, McCulley JP, Den S, Foulks GN: The international workshop on meibomian gland dysfunction: report of the definition and classification subcommittee. Invest Ophthalmol Vis Sci 2011, 52:1930−1937
34. Craig JP, Nichols KK, Akpek EK, Caffery B, Dua HS, Joo CK, Liu Z, Nelson JD, Nichols JJ, Tsubota K, Stapleton F: TFOS DEWS II definition and classification report. Ocul Surf 2017, 15:276−283
35. Janani C, Ranjitha Kumari BD: PPAR gamma gene–a review. Diabetes Metab Syndr 2015, 9:46−50
36. Guo Y, Zhang H, Zhao Z, Luo X, Zhang M, Bu J, Liang M, Wu H, Yu J, He H, Zong R, Chen Y, Liu Z, Li W: Hyperglycemia induces meibomian gland dysfunction. Invest Ophthalmol Vis Sci 2022, 63:30
37. Kim CE, Kleinman HK, Sosne G, Ousler GW, Kim K, Kang S, Yang J: RGN-259 (thymosin β4) improves clinically important dry eye efficacies in comparison with prescription drugs in a dry eye model. Sci Rep 2018, 8:10500
38. Zhang P, Li T, Wu X, Nice EC, Huang C, Zhang Y: Oxidative stress and diabetes: antioxidative strategies. Front Med 2020, 14:583−600
39. Kalogeris T, Bao Y, Korthuis RJ: Mitochondrial reactive oxygen species: a double edged sword in ischemia/reperfusion vs preconditioning. Redox Biol 2014, 2:702−714
40. Meneray MA, Fields TY: Adrenergic stimulation of lacrimal protein secretion is mediated by G(q/11)alpha and G(s)alpha. Curr Eye Res 2000, 21:602−607
41. Walcott B, Matthews G, Brink P: Differences in stimulus induced calcium increases in lacrimal gland acinar cells from normal and NZB/NZW F1 female mice. Curr Eye Res 2002, 25:253−260
42. Ding C, Walcott B, Keyser KT: Sympathetic neural control of the mouse lacrimal gland. Invest Ophthalmol Vis Sci 2003, 44:1513−1520
43. Iyngkaran P, Anavekar N, Majoni W, Thomas MC: The role and management of sympathetic overactivity in cardiovascular and renal complications of diabetes. Diabetes Metab 2013, 39:290−298
44. Huang C, Rosencrans RF, Bugescu R, Vieira CP, Hu P, Adu-Agyeiwaah Y, Gamble KL, Longhini A, Fuller PM, Leinninger GM, Grant MB: Depleting hypothalamic somatostatinergic neurons recapitulates diabetic phenotypes in mouse brain, bone marrow, adipose and retina. Diabetologia 2021, 64:2575−2588
45. Schlaich M, Straznicky N, Lambert E, Lambert G: Metabolic syndrome: a sympathetic disease. Lancet Diabetes Endocrinol 2015, 3:148−157
46. Fusco F, Palmieri A, Ficarra V, Giannarini G, Novara G, Longo N, Verze P, Creta M, Mirone V: α1-Blockers improve benign prostatic obstruction in men with lower urinary tract symptoms: a systematic review and meta-analysis of urodynamic studies. Eur Urol 2016, 69:1091−1101
47. Szarka D, Elekes G, Berczeli O, Vizvári E, Szalay L, Ding C, Tálosi L, Tóth-Molnár E: Alpha-adrenergic agonists stimulate fluid secretion in lacrimal gland ducts. Invest Ophthalmol Vis Sci 2020, 61:3
48. Ikeda-Kurosawa C, Higashio H, Nakano M, Okubo M, Satoh Y, Kurosaka D, Saino T: α1-Adrenoceptors relate Ca(2+) modulation and protein secretions in rat lacrimal gland. Biomed Res 2015, 36:357−369
49. Proctor GB, Carpenter GH: Regulation of salivary gland function by autonomic nerves. Auton Neurosci 2007, 133:3−18
50. Yoshino Y, Imamura T, Yamachika S, Ohshima T, Ushikoshi-Nakayama R, Inoue H, Saito I, Nakagawa Y: Endoplasmic reticulum stress affects mouse salivary protein secretion induced by chronic administration of an α(1)-adrenergic agonist. Histochem Biol 2022, 157:443−457
51. Kowluru RA: Mitochondrial stability in diabetic retinopathy: lessons learned from epigenetics. Diabetes 2019, 68:241−247
52. Pinti MV, Fink GK, Hathaway QA, Durr AJ, Kunovac A, Hollander JM: Mitochondrial dysfunction in type 2 diabetes mellitus: an organ-based analysis. Am J Physiol Endocrinol Metab 2019, 316:E268−E285
53. Reynoso-Paz S, Leung PS, Van De Water J, Tanaka A, Munoz S, Bass N, Lindor K, Donald PJ, Coppel RL, Ansari AA, Gershwin ME: Evidence for a locally driven mucosal response and the presence of mitochondrial antigens in saliva in primary biliary cirrhosis. Hepatology 2000, 31:24−29
54. Bertolini I, Ghosh JC, Kossenkov AV, Mulugu S, Krishn SR, Vaira V, Qin J, Plow EF, Languino LR, Altieri DC: Small

extracellular vesicle regulation of mitochondrial dynamics reprograms a hypoxic tumor microenvironment. Dev Cell 2020, 55: 163−177.e6

55. Hong Y, Tak H, Kim C, Kang H, Ji E, Ahn S, Jung M, Kim HL, Lee JH, Kim W, Lee EK: RNA binding protein HuD contributes to β-cell dysfunction by impairing mitochondria dynamics. Cell Death Differ 2020, 27:1633−1643
56. Wakamatsu TH, Dogru M, Matsumoto Y, Kojima T, Kaido M, Ibrahim OM, Sato EA, Igarashi A, Ichihashi Y, Satake Y, Shimazaki J, Tsubota K: Evaluation of lipid oxidative stress status in Sjögren syndrome patients. Invest Ophthalmol Vis Sci 2013, 54: 201−210
57. Čejková J, Čejka Č: The role of oxidative stress in corneal diseases and injuries. Histol Histopathol 2015, 30:893−900
58. Bhatti JS, Bhatti GK, Reddy PH: Mitochondrial dysfunction and oxidative stress in metabolic disorders - a step towards mitochondria based therapeutic strategies. Biochim Biophys Acta Mol Basis Dis 2017, 1863:1066−1077